Electrochimica Acta 490 (2024) 144305

Contents lists available at ScienceDirect

Electrochimica Acta

journal homepage: www.journals.elsevier.com/electrochimica-acta

Cresyl violet electropolymerization on functionalized multiwalled carbon nanotubes in carboxylic acid based ternary deep eutectic solvents for hydroquinone sensing

Rafael M. Buoro [a,b], Joseany M.S. Almeida [a], Christopher M.A. Brett [a,*]

[a] Department of Chemistry, CEMMPRE, ARISE, Faculty of Sciences and Technology, University of Coimbra, 3004-535 Coimbra, Portugal
[b] Departamento de Química e Física Molecular, Instituto de Química de São Carlos, Universidade de São Paulo, 13566-590 São Carlos, SP, Brazil

ARTICLE INFO

Keywords:
Cresyl violet
Ternary deep eutectic solvents
Multiwalled carbon nanotubes
Electropolymerization
Hydroquinone

ABSTRACT

The phenazine dye cresyl violet (CVio) has been evaluated as precursor for the preparation of a new electrochemical sensor based on poly(cresyl violet) deposited on multiwalled carbon nanotube (CNT) modified glassy carbon electrodes (GCE) in neutralized acid-doped ternary deep eutectic solvents (DES). DES with choline chloride as hydrogen bond acceptor and with different hydrogen bond donors (HBD), namely acetic acid, ethylene glycol and oxalic acid were evaluated for CVio electropolymerization by potential cycling. The best polymer films were obtained in ternary DES with the two HBD acetic acid plus ethylene glycol doped with H_2SO_4 and followed by NaOH neutralization. Electrochemical characterization (voltammetric and electrochemical impedance) showed the formation of anthraquinone groups during electropolymerization, which is initiated on the CNT by the formation of a cation radical. Anthraquinones in the polymer film led to an increased response at the modified electrode for the determination of hydroquinone (H_2Q) with low LOD (0.25 μmol L^{-1}) in a broad linear range (1–80 μmol L^{-1}), with good reproducibility, repeatability, and stability. The sensor was successfully applied to the quantification of H_2Q in dermatological creams with no matrix effect towards hydroquinone response.

1. Introduction

Conducting polymers are widely known for their electrochemical applications due to their role in enhancing sensitivity, selectivity, and electrocatalytic activity [1]. The polymer electronic conductivity is associated with a π* orbital conjugation which allows the delocalization of electrons through the polymeric structure [2]. Among the possible procedures to obtain conducting polymers, electropolymerization remains a simple yet efficient way to control the experimental conditions required to obtain a conducting polymer film with the desired properties [3]. Electropolymerization of phenazine dyes leads to polyphenazine-modified electrodes, the behaviour of which is based on the polymer redox activity [4–6]. The phenazine dye cresyl violet (CVio), used in neurobiology to highlight neuronal tissue, is composed of 4 aromatic rings, with the central one consisting of an O-N conjugated system. Due to its structural similarity with Nile blue, which has been reported to undergo electropolymerization [7], it is expected that CVio polymer formation (PCVio) will occur via C-N coupling once the cation radical initiator is formed at the electrode surface.

One of the several physicochemical properties of an electropolymerization solution that can be controlled is the medium composition, which can dramatically influence the polymer's electrochemical properties [7]. Recently, deep eutectic solvents (DES) have drawn attention as a reaction medium for material synthesis, including the preparation of conductive/redox polymers by increasing their stability and structural organization [8]. DES comprise two (binary) or more (tertiary for three) components: a hydrogen bond acceptor (HBA), molecules with highly electronegative groups that have a lone electron pair that can participate in a hydrogen bond, and a hydrogen bond donor (HBD), molecules with a functional group with a hydrogen atom bonded to a highly electronegative atom (F, O or N) [9–11]. Hydrogen bonds are established between the two components, appropriate component ratios promoting the formation of an eutectic mixture with a melting point significantly lower than that of the individual components [9]. Low toxicity, simple preparation, biodegradability, wide potential window, and low cost are DES characteristics commonly referred to, making them

* Corresponding author.
E-mail address: cbrett@ci.uc.pt (C.M.A. Brett).

https://doi.org/10.1016/j.electacta.2024.144305
Received 19 March 2024; Received in revised form 19 April 2024; Accepted 19 April 2024
Available online 20 April 2024

advantageous compared to ionic liquids [10,12,13] . Choline chloride (ChCl) based deep eutectic solvents have been widely used as HBA due to the low cost and low toxicity of ChCl [13–17]. Due to these characteristics, DES have been used to manufacture specific products in organic synthesis [18], as media for nanomaterial preparation [12,19] and composite electrodes [20], and in electropolymerization to prepare conducting and redox polymers for sensor applications [21]. In particular, polyphenazine dye modified electrodes have been successfully prepared in DES (binary or ternary) for the development of electrochemical sensors [6–8,22,23].

Although DES have a lower toxicity than ionic liquids, petroleum derivatives such as ethylene glycol (EG), present in the DES ethaline (ChCl:EG 1:2 ratio) are often used in electropolymerization procedures [4,5], opening up possibilities for even "greener" alternatives. Natural deep eutectic solvents (NADES) are a class of DES in which all components in the eutectic mixture are biocompatible and have low toxicity [14,15,21,24,25]. Within this category, choline chloride with oxalic acid (OA) [24] or acetic acid (AcA) [25] NADES have been successfully used for natural product extraction [25–30], plasticizers [24] and as media for organic synthesis [18,31]. Since ternary DES have been shown to improve the electropolymerization process [6,22], both binary and ternary mixtures based on both these acids are worth investigating to reduce the use of EG in the final eutectic solvent composition.

This article presents the development, electrochemical characterization, and application of a new modified electrode architecture based on the redox polymer PCVio prepared by electropolymerization in choline chloride-based DES, evaluating three different HBD: EG, OA, and AcA, in binary and ternary compositions. Modification of glassy carbon electrodes (GCE), the substrate in this study, by functionalised CNT increases the currents during electropolymerization owing to the larger surface area and CNT longitudinal electronic conduction [32–34]. It enables a sufficient amount of the cation radical initiator to start the polymerization [8,22]. The resulting polymer-modified CNT/GCE were characterized by cyclic voltammetry (CV), electrochemical impedance spectroscopy (EIS) and scanning electron microscopy (SEM). The sensor was applied to the quantification of hydroquinone (H_2Q), a phenolic derivative present in skin-lightening creams for the treatment of melasma [35,36]. To the best of our knowledge, the combination of DES electrodeposited CVio and CNT is a novel approach for the development of H_2Q sensors by more sustainable and simple procedures.

2. Experimental

2.1. Reagents and solutions

Reagents were all analytical grade and were used without further purification. Choline chloride, chitosan from crab shells (minimum 85 % deacetylated), ethylene glycol 99.8 %, sulfuric acid (95 %), hydrochloric acid (37 %), perchloric acid (70 %), acetic acid (99.98 %) hydroquinone and di-sodium hydrogen phosphate heptahydrate ($Na_2HPO_4{\cdot}7H_2O$) were acquired from Sigma-Aldrich, Germany. Cresyl violet monomer (CVio) P.A. was obtained from Carl Roth, Germany. Oxalic acid dihydrate was obtained from Fluka, Switzerland. Boric acid (H_3BO_3) and sodium hydroxide, pellets (NaOH) were obtained from J.T. Baker, USA. Sodium dihydrogen phosphate (NaH_2PO_4) was obtained from Riedel-de-Haën, Germany. Multiwalled CNT were acquired from Nanolab, USA with ~95 % purity, length 1–5 μm and outer diameter 30 ± 10 nm.

Electrochemical characterization of the polymer-modified electrodes in aqueous media was carried out in Britton-Robinson (BR) buffer solution, pH 3.0, prepared by mixing acetic acid, boric acid and phosphoric acid in 0.04 mol L^{-1} concentration and adjusting the pH to the desired value with a 5.0 mol L^{-1} NaOH solution. Millipore Milli-Q nanopure water (resistivity ≥ 18.2 MΩ cm) was employed for preparing all solutions. All experiments were performed at room temperature (25 ± 1 °C).

2.2. Instrumentation

Voltammetric experiments were carried out using an Ivium nStat potentiostat (software version 2.024, Ivium Technologies, Netherlands) with a conventional 3-electrode electrochemical cell. A GCE (geometric area = 0.00785 cm^2), a 3 mm diameter Pt coated/Ti rod and an Ag/AgCl (3 M KCl) electrode were used as working, counter and reference electrode respectively, all from eDAQ, Australia. Before each electrochemical experiment, the GCE surface was polished with 3 μm particle size diamond spray (Kemet, UK), followed by rinsing the surface with Milli-Q water to remove all adsorbed diamond particles. All currents were normalized by the GCE geometric area to facilitate the comparison and contextualization of the obtained results.

Electrochemical impedance measurements were carried out with a Solartron 1250 Frequency Response Analyzer coupled to a Solartron 1286 Electrochemical Interface controlled by the Zplot 2.4 software (Solatron Analytical, Ametek, UK). A sinusoidal voltage perturbation of amplitude 10 mV rms was applied in the frequency range from 65 kHz to 0.1 Hz with 10 frequencies per frequency decade. ZView software (version 2.4, Scribner Associates, USA) was used to fit the spectra to equivalent electrical circuits.

The morphological characterization of the modified electrodes was carried out with a scanning electron microscope (SEM) (GeminiSEM 460, ZEISS, Germany) operating at an acceleration voltage of 1 kV using carbon film electrode (CFE) substrates made from electrical resistors, with an exposed area of 0.020 cm^2. The pH measurements were performed using an Edge® HI2002–02 pHmeter (Hanna Instruments, Woonsocket, Rhode Island, USA).

2.3. Functionalization of multiwalled carbon nanotubes and electrode modification

The CNT were functionalized, due to their hydrophobic nature, in 5.0 mol L^{-1} HNO_3 under mechanical stirring for 24 h, filtered with 0.3 μm paper, and rinsed with Milli-Q nanopore water and then dried overnight at 80 °C. 100 mg of chitosan powder was dissolved in 10 mL of 1.0 % v/v acetic acid under vigorous stirring until a homogeneous 1 % (w/v) chitosan solution was obtained. A CNT dispersion in chitosan was prepared by mixing 10 mg of CNT in 1.0 mL of the chitosan solution under sonication (frequency 40 kHz, sonication power 60 W, Vevor, Spain) for 3 h to obtain a homogenous dispersion. Finally, 2 μL of the CNT dispersion was drop cast on the freshly polished GCE surface and dried overnight (16 h) at room temperature.

2.4. DES and nades synthesis and preparation by electropolymerization of PCVio/CNT/GCE modified electrodes in binary and ternary eutectic mixtures

All binary mixtures (ethaline 1ChCl:2EG, ChCl:OA 1:1 and ChCl:AcA: H_2O 1:2:2) were prepared following the same procedure. ChCl was previously heated to 60 °C under manual stirring for 5 min to eliminate crystallization water. The HBD was then added, and the mixture was vigorously stirred until a clear and homogeneous mixture was obtained. The three binary eutectic mixtures were stored at room temperature. The ternary mixtures were prepared by mixing two of the three binary mixtures with different HBD in a 1:1 V/V ratio to produce tDES1 (1ChCl:1EG:0.5OA), tDES2 (1ChCl:1EG:1AcA:1H_2O) and tDES3 (1ChCl:1AcA:0.5OA:1H_2O).

Films of PCVio were formed by potential cycling electropolymerization on GCE and CNT/GCE in the chosen DES containing 1.0 mmol L^{-1} CVIo. Acid dopants were added by the dropwise addition of an appropriate volume of concentrated H_2SO_4 or of another mineral acid when stated (HCl or $HClO_4$), under stirring. Similarly, neutralized solutions were prepared with the dropwise addition of an appropriate volume of 10 mol L^{-1} NaOH to the acid-doped CVio monomer solutions. Neutralized solutions were also evaluated as previous work suggests

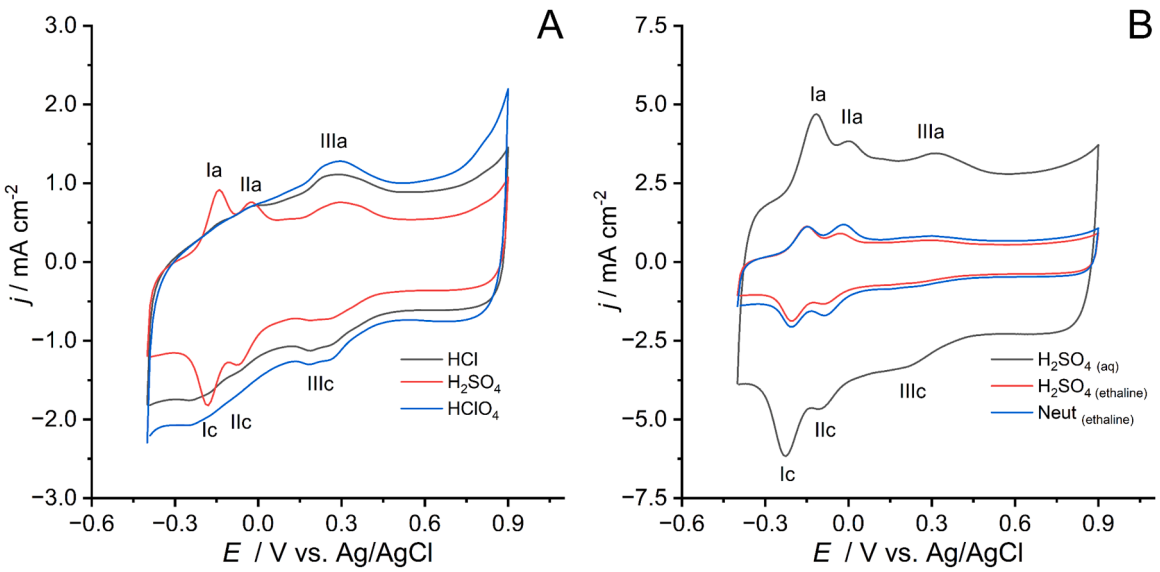

Fig. 1. pH 3.0 BR buffer electrochemical response of the PCVio films prepared: (A) using different acid dopants; (B) in acidic (H_2SO_4) and neutralized ethaline and aqueous solutions.

them to be a suitable medium for electropolymerization [7]. All CVio solutions were sonicated after the dopant addition for 10 min to ensure monomer dissolution. The potential range applied for the procedure was −0.4 to +0.9 V vs. Ag/AgCl, during 15 scans, at a scan rate of 50 mV s^{-1} unless stated otherwise.

The characterization of PCVio film modified electrodes was performed in BR buffer solution pH 3.0, in the potential range −0.4 to 0.9 V vs Ag/AgCl, at a scan rate of 50 mV s^{-1}. The differential pulse voltammetry (DPV) electrochemical characterization and the analytical determination of H_2Q, carried out in triplicate, were performed with the following parameters: pulse amplitude 25 mV, pulse time 250 ms, potential step 2 mV and scan rate 4 mV s^{-1}.

2.5. Hydroquinone determination in pharmaceutical samples

Samples of 0.1000 g of pharmaceuticals containing H_2Q, available in gel formulation and acquired in local pharmacies were dissolved in the supporting electrolyte (phosphate buffer 0.1 mol L^{-1}, pH 2.0) in a 25.00 ml volumetric flask. For the complete extraction and solubilization of the analyte, the sample mixture was sonicated in an ultrasound bath for 10 min. The final sample solutions were diluted in the electrochemical cell to adjust the H_2Q concentration to the linear range of the respective calibration curve.

3. Results and discussion

3.1. Cresyl violet (CVio) electropolymerization on CNT in different des and voltammetric behaviour of PCVio films

Electropolymerization of CVio was first carried out on bare GCE in ethaline with and without acid dopant, as previous studies demonstrated ethaline as a suitable medium for electropolymerization [7]. The potential cycling response showed no evidence of polymerization since the electrochemical signal did not increase with increasing number of scans (Fig. S1 A, B). CNT/GCE electrodes, however, presented a substantial increase of peak currents with increasing number of cycles in the presence of a dopant, see below.

The cyclic voltammograms presented in Fig. 1A, B illustrate the BR buffer electrochemical response of $PCVio_{ethaline}$ with three different 1.0 mol L^{-1} acid dopant solutions, namely H_2SO_4, HCl and $HClO_4$. The corresponding polymerization profiles are shown in Fig. S2A–C.

Better-defined and higher current peaks of a reversible redox couple were observed when H_2SO_4 was used as dopant. The polymerization mechanism proposed occurs by a similar pathway to that of Nile blue due to its similar chemical structure [7], with the formation of a cation radical followed by nucleophilic amine addition. However, as ethaline is hygroscopic [37] and due to the anthracene-like aromatic structure of CVio, H_2O may act as a nucleophile with the formation of quinone derivatives after cation radical formation. Anthracene was reported to undergo oxidation at relatively low potentials (+0.9 V) in activated carbon pores to produce anthraquinone derivatives [38]. The observed potentials for the peaks of PCVio films are similar to those observed for anthracene oxidation and are in the potential range for anthraquinone (AQ) structures [38]. CNT can act in a similar way as the porous activated carbon and allow the formation of AQ couples at high positive potentials.

The three redox couples observed (Ia/Ic, IIa/IIc and IIIa/IIIc) can be associated with quinone groups since they have similar peak potentials as anthraquinone derivatives [38,39], suggesting the formation of AQ groups during the polymerization process. The same redox processes can be observed at the $PCVio_{aqueous}$ film, Fig. S2A, C, when polymerization is performed in a 1.0 mol L^{-1} H_2SO_4 monomer solution, although a much higher capacitive current is observed for $PCVio_{aqueous}$ in the buffer response, Fig. 1B.

To understand the role of H^+ in the PCVio electrochemical behaviour, the polymerization was carried out in a H_2SO_4-ethaline neutralized solution which presented the same 3 redox couples observed in $PCVio_{ethaline}$ with higher currents than when acidic ethaline was used, demonstrating that the presence of extra electrolyte ions is more important for the polymerization in ethaline than acidic catalysis. However, the acid catalysis is necessary in aqueous solutions since no polymerization was observed in neutral Na_2SO_4 aqueous solution. Na_2SO_4 ethaline solutions, formed directly, were also considered as possible neutral media for PCVio formation. However, addition of the acid in the first step is essential to completely dissolve the CVio monomer.

The other two neutralized binary mixtures, i.e. neutralized ChCl:AA: H_2O 1:2:2 and ChCl:OA 1:1, were also evaluated as possible binary mixtures for PCVio electropolymerization. However, the high viscosity of ChCl:AA:H_2O 1:2:2 [40] and the crystallization of the ChCl:OA 1:1 solution with monomer at temperatures below 20 °C hindered the use of these binary mixtures for electropolymerization.

The H_2SO_4 neutralized ternary mixtures tDES1, tDES 2 and tDES3 were then evaluated for the electropolymerization of PCVio under the

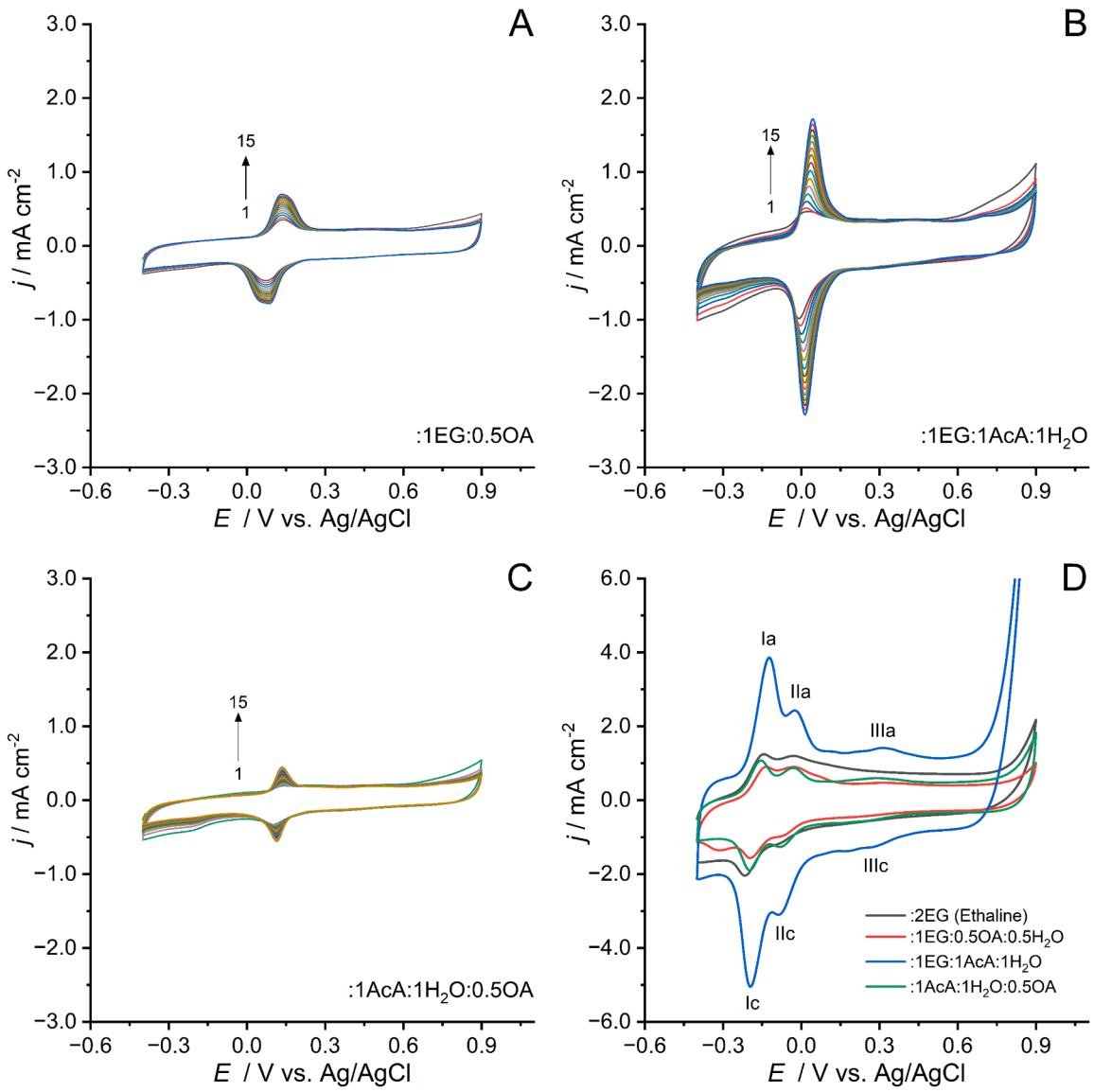

Fig. 2. Potential cycling electrodeposition of PCVio films on CNT/GCE at a scan rate of 50 mV s^{-1}, containing 1.0 mmol L^{-1} CVio in: (A) tDES 1, (B) tDES2, (C) tDES3 as medium. (D) pH 3.0 BR buffer electrochemical response of the PCVio films. All DES proportions displayed were normalized to 1 part of ChCl.

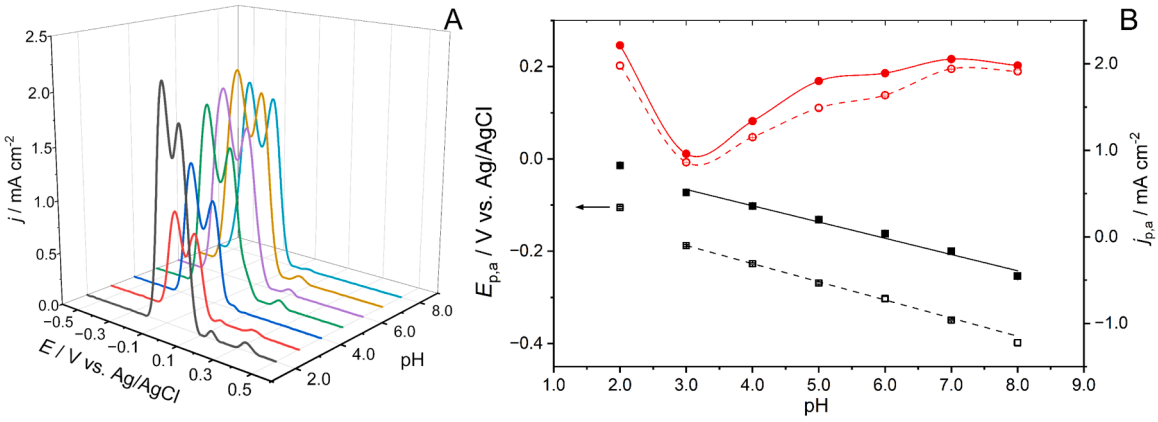

Fig. 3. DPVs of $PCVio_{tDES2}$/CNT/GCE modified electrodes in 0.1 mol L^{-1} BR buffer solution from pH 2.0 to 8.0; (B) plots of oxidation peak currents and peak potentials vs. pH, data from Figure 3A.

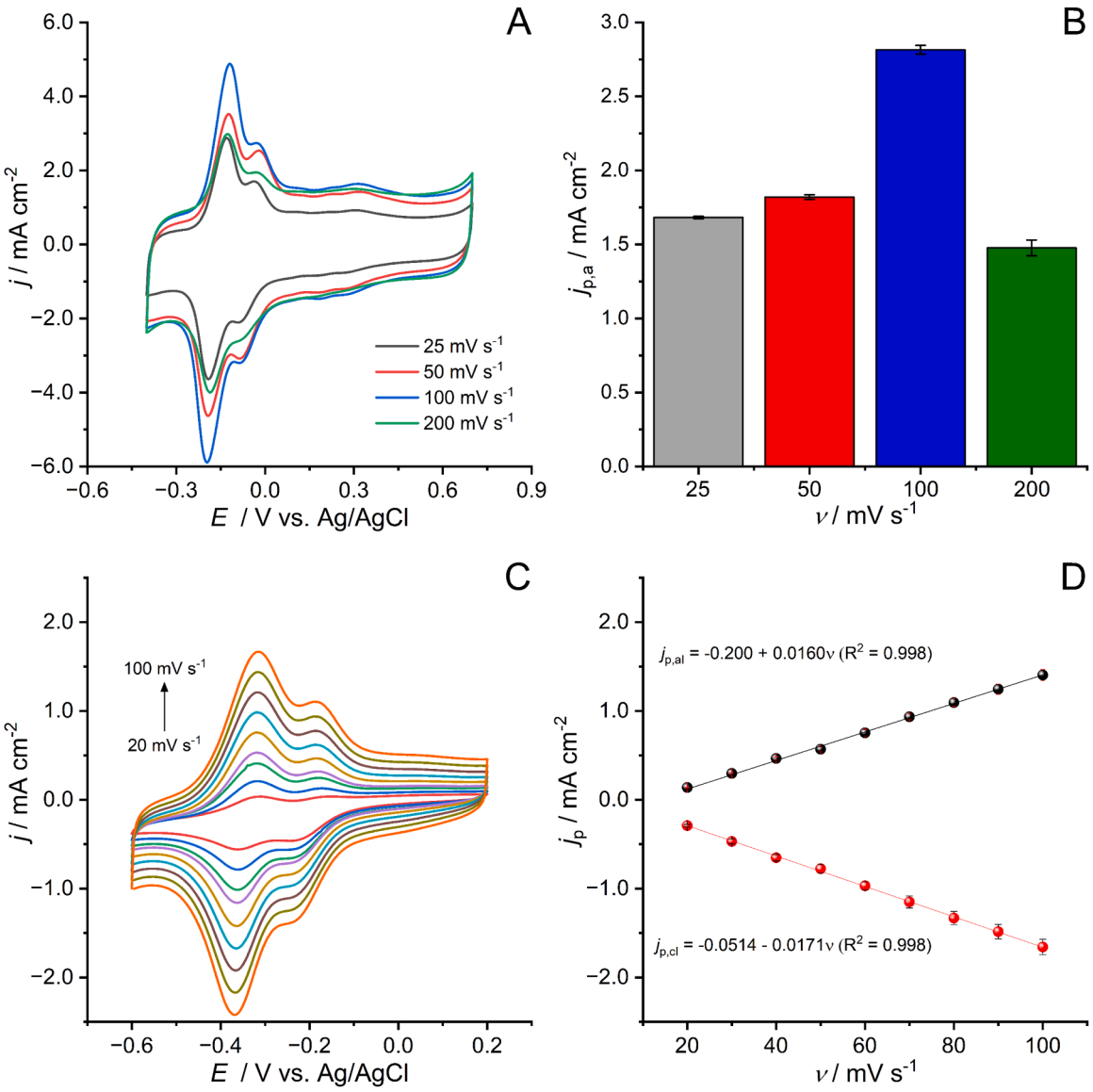

Fig. 4. (A) Cyclic voltammograms of PCVio$_{tDES2}$/CNT/GCE in 0.1 mol L^{-1} BR buffer pH 3.0 with different polymerization scan rates in DES and (B) the corresponding anodic peak currents. (C) Cyclic voltammograms at PCVio$_{tDES2}$/CNT/GCE in 0.1 mol L^{-1} BR buffer pH 3.0 for different scan rates and (D) corresponding plot of $j_{p,a}$ and $j_{p,c}$ vs scan rate, ν.

same conditions as ethaline. The tDES2 (1ChCl:1EG:1AA:1H_2O) presented the highest current peaks for the redox couples indicating a larger amount of anthraquinone groups in the polymer film. Since quinone groups can act as redox mediators, PCVio$_{tDES2}$ was seen to be more suitable for sensing applications. A shift of the peak potentials to less positive values during electropolymerization can be observed for CVio films prepared in tDES2 ($E_{p,a}$ = 0.044 V), Fig. 2B, compared to tDES1 and tDES3 ($E_{p,a}$ = 0.133 V for both tDES1 and tDES3), Fig. 2A and 2C, where oxalic acid is one of the HBD. The pH of the ternary mixtures was measured with pH strips, obtaining values between 0 and 1 for both oxalic acid mixtures and between 2 and 3 for the tDES2. The pH values are in line with the pK_a of OA (1.28 and 4.28) and AcA (4.75) observed in aqueous media [41]. The potential shift is more evident in neutralized ethaline ($E_{p,a}$ = - 0.205 V), Fig. S2E, than for the acid doped ethaline and aqueous polymerization, Fig. S2D.

The influence of potential cycling scan rate during polymer formation was also evaluated, with scan rates of 25, 50, 100 and 200 mV s^{-1}. A scan rate of 100 mV s^{-1} led to the highest current peaks. These results will be further discussed below in Section 3.2 along with other electrochemical properties of the PCVio$_{tDES2}$/CNT/GCE.

3.2. Electrochemical characterization of the PCVio$_{tdes2}$/CNT/GCE

The electrochemical response of PCVio$_{tDES2}$/CNT/GCE showed a pH-dependent behaviour with negative potential shifts of all peaks with increasing pH, Fig. 3A, B. Peaks Ia and IIa followed the equations $E_{p,aI}$ = −0.0698 – 0.03923 pH (R^2 = 0.996) and $E_{p,aII}$ = 0.0395 – 0.03521 pH (R^2 = 0.982) indicating a greater involvement of electrons than protons in the electrochemical process.

The deconvolution of the differential pulse voltammogram obtained with PCVio$_{tDES2}$/CNT/GCE in pH 3.0 BR buffer shows no influence of peak IIa on peak potential Ia, Fig. S3. Although many anthraquinone structures present a −59 mV/pH unit slope in the E_p vs pH plot [38], the H^+ availability could be limited due to the polymeric structure being confined to the CNT network which makes diffusion of H^+ to inner parts of the PCVio/CNT modifier layer difficult. The impedance spectra in Section 3.3 will provide more information regarding this matter. Peak current values increase with higher pH except in highly acidic medium, pH 2.0, where a maximum current density (2.21 ± 0.02 mA cm^{-2}) is observed.

The effect of scan rate during polymerization on the voltammetric

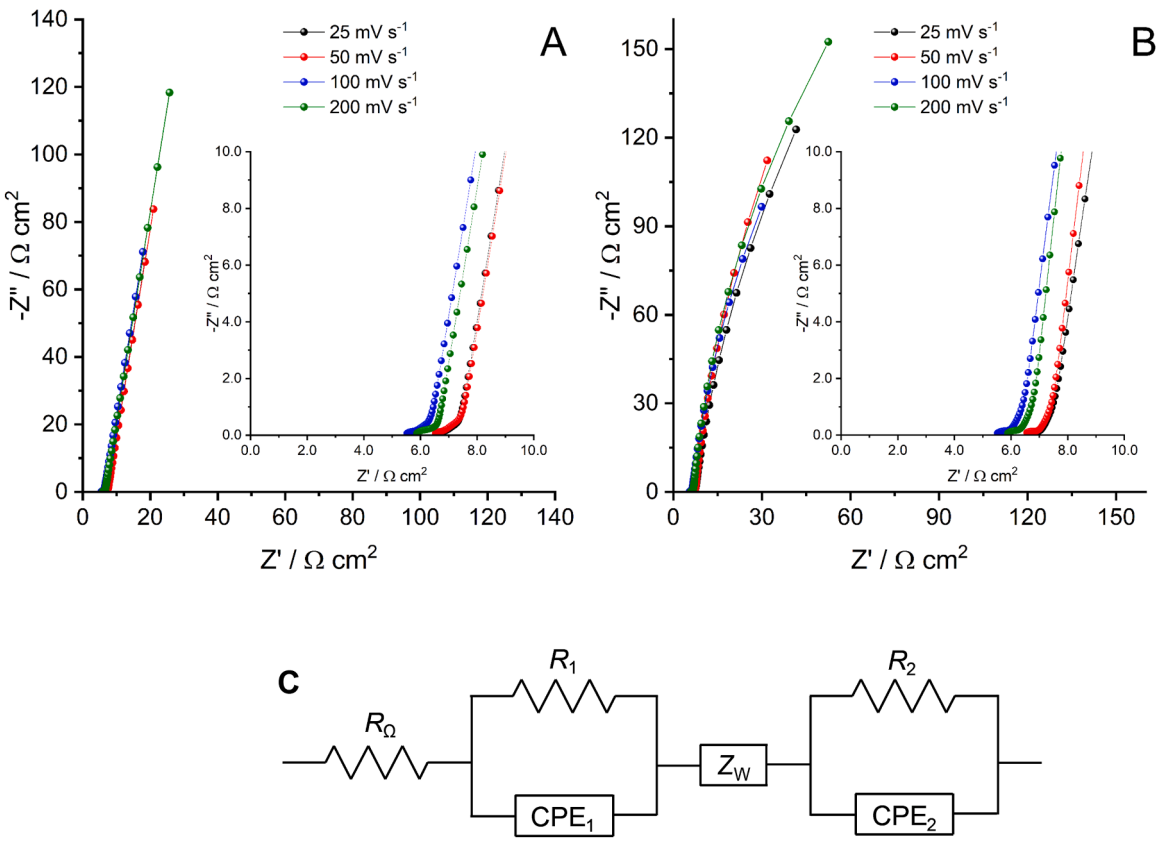

Fig. 5. Complex plane impedance spectra obtained at PCVio$_{tDES2}$/CNT/GCE in pH 3.0 BR buffer solution at different scan rates. The insets in the spectra show the high frequency region. (A) $E = -0.16$ V ($E_{1/2}$ of Ia/Ic) and (B) $E = -0.04$ V ($E_{1/2}$ of IIa/IIc) vs Ag/AgCl. (C) Electrical equivalent circuit used to fit the spectra.

profile as well as on the response of the assembled PCVio$_{tDES2}$CNT/GCE in 0.1 mol L^{-1} BR buffer was investigated. The cyclic voltammograms in Fig. 4A showed higher peak currents when polymerization is performed at 100 mV s^{-1}, Fig. 4B. This could be related to the number of polymer initiators caused by the oxidation CVio to its cation radical without further oxidation of its structure. At lower scan rates, the formed cation radicals can be further oxidized to a non-reactive molecule. This conclusion is corroborated by the increase of the current peaks in PCVio$_{tDES2}$ films when the scan rate is gradually increased from 25 to 100 mV s^{-1}. The higher the scan rate, the more important are diffusion limitations, reducing the amount of cation radicals to initiate the polymerization and of monomers for polymer growth. Above 100 mV s^{-1}, the effect of this is that the peak currents diminish in height besides which the electrode is kept for a shorter period of time within the potential range where the cation radicals are formed, between + 0.7 and 0.9 V.

Fig. 4D shows linear relationships between PCVio$_{tDES2}$ peak currents in Fig. 4C and scan rate which is typical for adsorption controlled electrochemical processes and confirming the polymerization of CVio on the CNT/GCE surface.

3.3. Electrochemical impedance spectroscopy (EIS)

The interfacial properties of PCVio$_{tDES2}$/CNT/GCE from polymerization at different scan rates were evaluated by EIS, carried out at E_{bias} of −0.16 V and −0.04 V chosen since they are the half wave potential observed in the CV for $E_{p,aI}/E_{p,cI}$ and $E_{p,aII}/E_{p,cII}$ respectively. The spectra at both E_{bias}, Fig. 5A and 5B presented a very small semi-circle at high to medium frequency ranges for all the scan rates evaluated. The equivalent circuit used to fit the impedance spectra presented in Fig. 5A is given in Fig. 5C and has been used for successful fitting of similar modified electrode architectures, e.g. [5,22]. It comprises the association of R_Ω (cell resistance) followed by R_1, associated with a charge transfer process at high frequency between the electrode surface and the modifier layer, in parallel with a constant phase element CPE$_1$ representing a non-ideal capacitor. The expression for CPE$_1$ is given by CPE = $1/(Ci\omega)^\alpha$ where C is the capacitance, ω is the angular frequency in rad s^{-1} and α varies between 0.5 and 1, the limits corresponding to

Table 1
Electrical equivalent circuit element values obtained from the fitted impedance spectra.

E / V vs. Ag/AgCl	ν / mV s^{-1}	R_1 / Ω cm^2	CPE$_1$ / mF cm^{-2} s$^{\alpha-1}$	α_1	Z_w / Ω cm^2	α_{Zw}	R_2 / Ω cm^2	CPE$_2$ / mF cm^{-2} s$^{\alpha-1}$	α_2
−0.16	25	0.29	2.1	0.67	0.025	0.46	–	–	–
	50	0.26	2.9	0.64	0.025	0.47	–	–	–
	100	0.26	3.3	0.64	0.025	0.47	–	–	–
	200	0.40	3.5	0.64	0.009	0.48	–	–	–
−0.04	25	0.45	2.1	0.58	0.059	0.44	516	14.7	0.92
	50	0.45	3.5	0.58	0.069	0.45	604	16.7	0.94
	100	0.45	4.8	0.58	0.082	0.45	447	18.9	0.95
	200	0.45	4.8	0.59	0.059	0.44	570	11.1	0.96

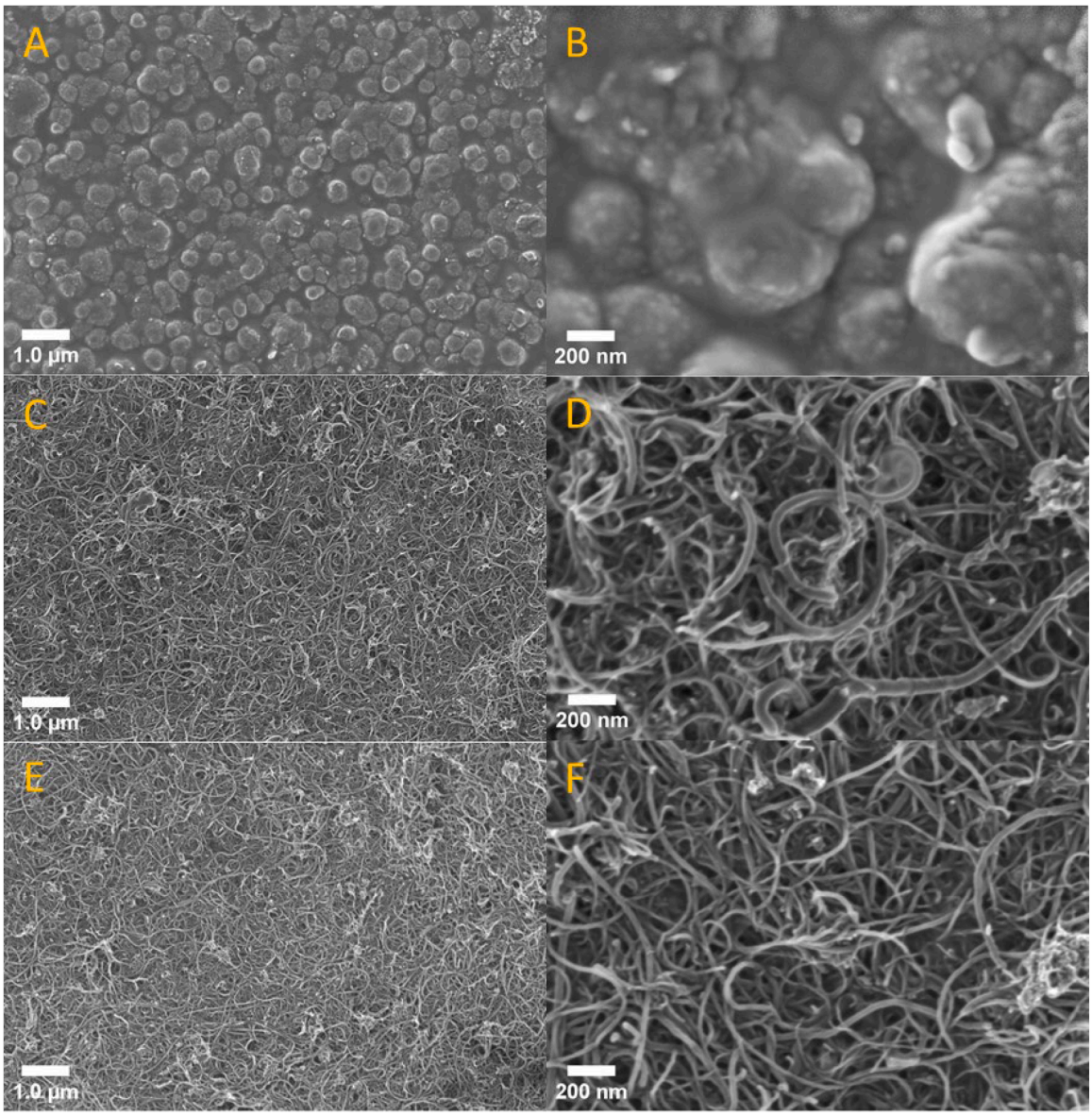

Fig. 6. SEM images of: CFE (A, B), CNT/CFE (C, D) and PCVio$_{tDES2}$/CNT/CFE (E,F).

rough/porous and to completely uniform modified electrodes. At medium frequencies, diffusion through the modified film is represented by a finite diffusion impedance, Z_W. Finally, the R_2CPE_2 combination at low frequencies represents charge transfer processes at the modifier layer / solution interface. Table 1 shows the values of the equivalent circuit parameters obtained by fitting.

The values of α observed in all spectra in the high frequency region feature are around 0.6 at both applied potentials, and can be associated with the large non-uniformity of the GCE-modifier film (CNT and PCVio) interface.

At medium frequencies, the linear increase of the diffusion impedance Z_W is attributed to finite diffusion within the PCVio/CNT films with an α_{ZW} value approaching 0.5 with the increasing scan rate. The values of Zw were constant up to 100 mV s^{-1} which indicates polymer films of similar thickness [42,43]. At 200 mV s^{-1}, the decrease in the Z_W value can be associated with a thinner polymer film since the applied potential is kept for less time within the potential region where the cation radical is formed, thence decreasing the polymerization rate.

At low frequencies, the start of a new semicircle can be observed at $E = -0.04$ V, for all scan rates evaluated, Fig. 5B, but not at −0.16 V. This is described by R_2CPE_2 in Fig. 5C, and corresponds to the modifier film-solution interface. When polymerization is done at 100 mV s^{-1}, it can be observed that the modified electrode has the lowest R_2 value (447 Ω cm^2, Table 1) and the highest capacitance (18.9 mF cm^{-2}), which can be associated with more AQ groups at the electrode surface. This helps to explain the increased peak currents observed in the cyclic voltammograms displayed in Fig. 4A, B. Finally, α_2 values approach 1 with increasing scan rate which suggests a more uniform charge transfer at the polymer film modifier-solution interface.

3.4. PCVio$_{tDES2}$/CNT film characterization by SEM

The PCVio$_{tDES2}$/CNT surface morphology was investigated by scanning electron microscopy using a carbon film electrode (CFE) as substrate. Although the CFE, Fig. 6A and B, exhibits an irregular surface with granulometric aspect, the CNT/CFE, Fig. 6C and D, presents uniform roughness and some porosity, seen as dark areas, associated with the network of the CNT film. After CVio polymerization on CNT, the PCVio$_{tDES2}$/CNT/CFE, Fig. 6E and F, these dark areas are filled with what can be associated with the PCVio polymeric structure. This

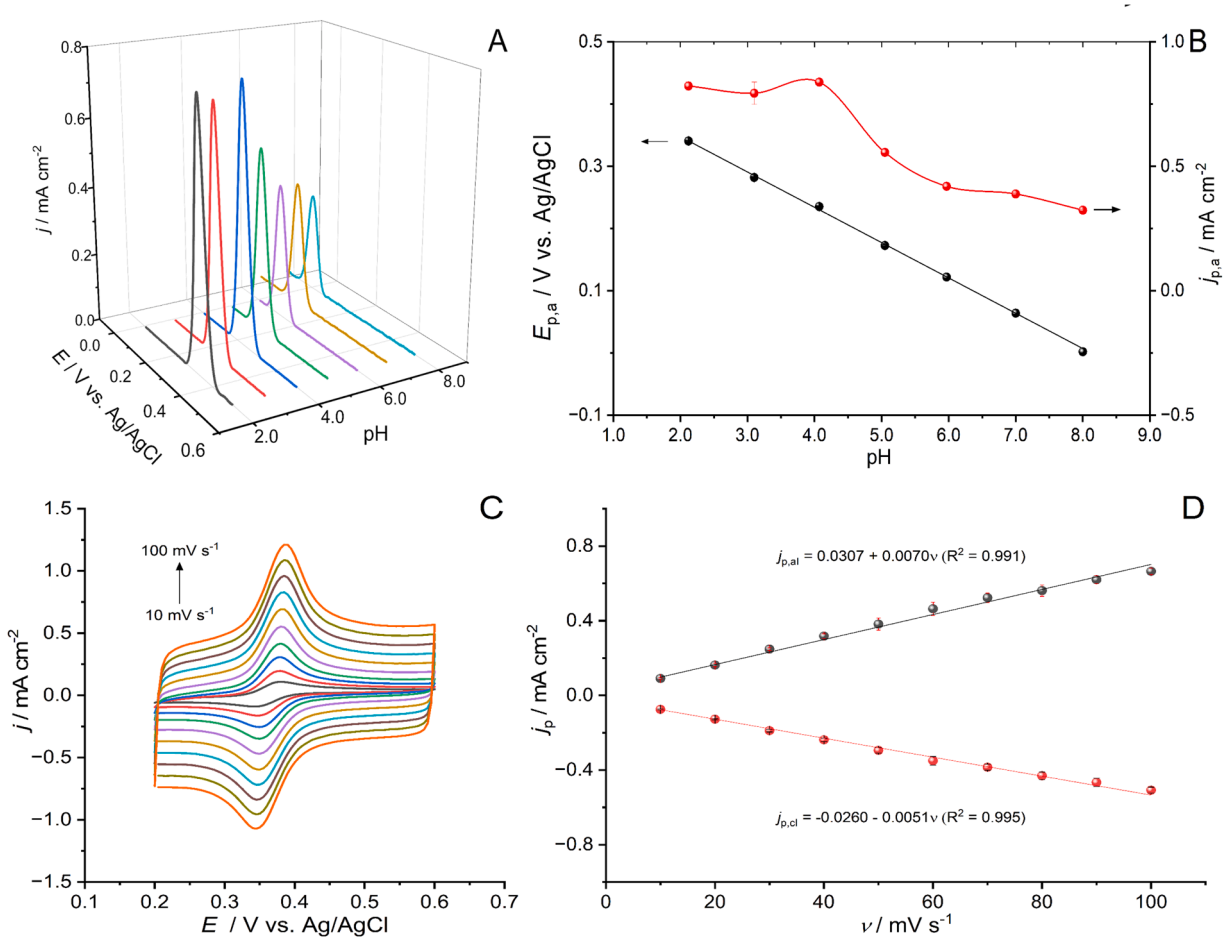

Fig. 7. (A) Baseline corrected differential pulse voltammograms obtained in a 100.0 μmol L^{-1} H_2Q solution in 0.1 mol L^{-1} phosphate buffer at different pH values with $PCVio_{tDES2}$/CNT/GCE (B) corresponding E_p/j_p vs pH plot. (C) Cyclic voltammograms obtained in a 100.0 μmol L^{-1} solution of H_2Q in phosphate buffer pH 2.0 on $PCVio_{tDES2}$/CNT/GCE at different scan rates and (D) corresponding plots of $j_{p,a}$ and $j_{p,c}$ vs scan rate, ν.

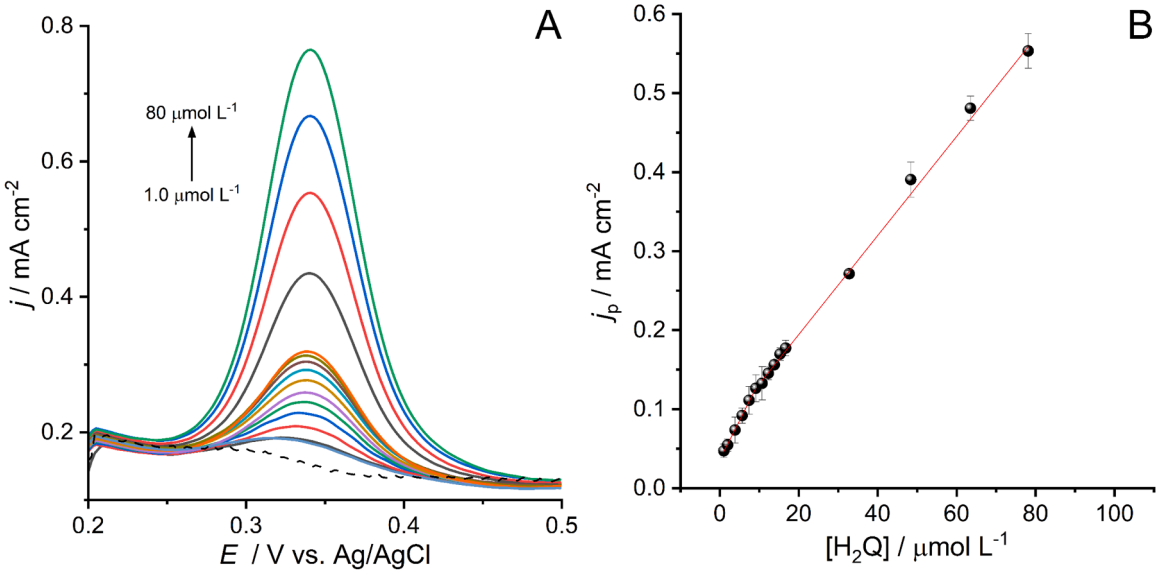

Fig. 8. (A) DPVs obtained with $PCVio_{tDES2}$/CNT/GCE in phosphate buffer pH 2.0 for 1.0 to 80 μmol L^{-1} and (B) corresponding calibration plot.

corroborates the hypothesis that PCVio polymerization is confined to the CNT network and promotes the formation of a film that fills the holes in the polymeric network and can hinder the diffusion of H^+ to inner parts of the PCVio/CNT modification, limiting the H^+ availability to AQ groups that are in the inner polymer layers.

Table 2
Electrochemical sensors for H_2Q sensing in the recent literature.

Sensor Architecture	Technique	LOD/ μmol L^{-1}	Linear Range / μmol L^{-1}	Sample	Refs.
$PSF_{Ethaline}$/MWCNT-CuO/PGE	DPV	0.3	1.5–100	Tap water/milk	[8]
DLC:VAMWCNT	FIA-Amperometry	0.77	1.0–100	Dermatological cream	[35]
HDES 6.0	SWAdASV	0.77	2.5–3000	Dermatological cream	[36]
Gr-COOH/GCE	AdASV	0.04	0.1–50	Whitening cream	[44]
$Au_3@Pd_6$/GCE	DPV	0.63	4–5000	Tap/lake water	[45]
Poly(Neutral Red)/P-Gr/GCE	AdSDPV	0.014	0.045–0.91 0.91–9.1 9.1–63.7	Whitening cream	[46]
Ce-MOF(TV)/ CNTs/GCE	DPV	5.3	10–100	River Water	[47]
Pt/C60/PGE	DPV	2.2	50–1100	River/sanitary wastewater	[48]
G-PBAT	DPV	1.0	0.1–1400	Dermatological cream	[49]
$PCVio_{tDES2}$/CNT/GCE	DPV	0.25	1–10 10–80	Dermatological cream	This work

GCE – Glassy carbon electrode; $PSF_{Ethaline}$/MWCNT/CuO/GCE – poly(safranine T)/MWCNT/copper oxide; DLC:VAMWCNT – diamond-like carbon film deposited on vertically aligned MWCNT; HDES 6.0 - Hydrophobic deep eutectic solvent carbon paste electrode; Gr-COOH/GCE - carboxylic acid-functionalized graphene; $Au_3@Pd_6$/GCE – Gold - Palladium core shells; Poly(neutral red)/P-Gr/GCE – poly(neutral red)/ porous graphene; Ce-MOF(TV)/CNTs/GCE – Cerium Metal Oxide Framework/carbon nanotubes; Pt/C60/PGE – Platinum/Fullerene; G-PBAT – graphite/poly(butylene adipate-co-terephthalate).

3.5. Optimization of $PCVio_{tdes2}$/CNT/GCE sensors for hydroquinone detection: pH and scan rate effect on H_2Q oxidation

In order to demonstrate application of the sensor, the electrochemical oxidation of hydroquinone was evaluated on the $PCVio_{tDES2}$/CNT/GCE at different pH values by DPV, assessing the optimal pH value for H_2Q analysis and the electrochemical behaviour of hydroquinone. The E_p/j_p plots vs pH showed pH 2.0 as the best condition for H_2Q oxidation with a current density (j) of 0.822 ± 0.016 mA cm^{-2}, Fig. 7A, B. The linear fitting for the E_p vs pH plot followed the equation $E_{p,a}$ = 0.461 – 0.057 pH (R^2 = 0.994) in agreement with a mechanism involving the same number of protons and electrons, as described in the literature [8,35]. The $j_{p,a/p,c}$ vs. ν plots were linear for all the scan rates studied indicating a predominantly adsorption-controlled process and suggests adsorption of H_2Q on the $PCVio_{tDES2}$/CNT/GCE surface prior to its oxidation via AQ groups interaction, Fig. 7C, D.

3.6. Analytical performance of $PCVio_{tdes2}$/CNT/GCE and interferences

The analytical performance of $PCVio_{tDES2}$/CNT/GCE was evaluated by varying the H_2Q concentration in the range from 1.0 to 150 μmol L^{-1}. As shown in Fig. 8, the peak current density increased linearly with increase in concentration of H_2Q, presenting two linear segments. The first linear segment, from 1.0 to 10 μmol L^{-1}, follows the linear regression equation j_1 (mA cm^{-2}) = 0.0362 + 0.0099 [H_2Q] (R^2 = 0.998, 1–10 μmol L^{-1}) with a sensitivity of 9.90 μA (μmol L^{-1})$^{-1}$ cm^{-2}. The second linear region is up to 80 μmol L^{-1} following the linear regression equation j_2 = (mA cm^{-2}) = 0.0692 + 0.00627 [H_2Q] (R^2 = 0.996, 10 – 80 μmol L^{-1}) with corresponding sensitivity of 6.27 μA (μmol L^{-1})$^{-1}$ cm^{-2}. The calculated limits of detection (LOD) and quantification (LOQ), (using 3σ/s and 10σ/s), were 0.25 μmol L^{-1} and 0.83 μmol L^{-1}, respectively. The current for H_2Q oxidation in a 50.0 μmol L^{-1} solution observed at PCVio/CNT/GCE is 75 times that at GCE and 15 % more than at CNT/GCE, Fig. S4A, B, which can be associated with the increase of the surface area promoted by the PCVio/CNT association. Besides this, the PCVio film improves electrode stability as can be inferred from triplicate measurements where triplicates had an RSD% of 0.30 %, lower than at CNT/GCE (RSD% = 3.0 %) and GCE (RSD% = 25 %). The higher RSDs observed for CNT/GCE and GCE are a consequence of the H_2Q peak current intensity reduction of over 7 % and 50 % respectively, after 3 successive measurements which evidences the protection against fouling from the PCVio film. Repeatability measurements below provide more data regarding this aspect. The PCVio film also causes a shift of H_2Q oxidation peak potential to less positive values. The higher sensitivity of the first linear segment at low H_2Q can be ascribed to the interaction of H_2Q to AQ groups formed during polymerization, the AQ groups being widely available to interact with H_2Q with no hindrance due to the low concentration of H_2Q. At high concentrations, however, H_2Q aggregates on the polymer film to form a multilayer-covered surface, due to the limitation from the number of active sites on the electrode surface. The adsorptive behaviour of H_2Q on $PCVio_{tDES2}$/CNT/GCE could potentially be explored using adsorptive stripping differential pulse voltammetry with an accumulation step at open circuit potential, increasing the sensitivity of the proposed method.

Analysing literature reports during the last 5 years, the proposed sensor presents LOD and LOQ within the same range as other H_2Q electrochemical sensors with more complex electrode modifications and/or time-consuming analytical methods, see Table 2, and without incorporating potentially toxic metallic materials.

To ascertain the selectivity of the proposed sensor, ascorbic acid (AA) was tested as a possible interferent to the determination of H_2Q with a concentration (100.0 μmol L^{-1}) 5-fold higher than H_2Q (20.0 μmol L^{-1}). Many formulations use AA as an antioxidant to avoid H_2Q oxidation to benzoquinone once the pharmaceutical product is exposed to oxygen. The RSD% of + 1.7 % between H_2Q and H_2Q in the presence of AA confirms that AA has no significant influence on the response of the proposed sensor. Inorganic species such as Ca^{2+}, Mg^{2+}, Na^{+}, Zn^{2+} Cl^{-}, NO_3^{-} and organic species, CH_3COO^{-}. EDTA, which is also present in many cosmetic formulations, in concentrations 10 times higher than H_2Q also had no influence (RSD_{max} =1.8 %). Other interferents such as BHT and emollients were not considered as potential interferents due to the hydrophobic nature of the molecules. BHT is an antioxidant commonly used in oil-based formulations and emollients are long chain esters also insoluble in aqueous solutions. Therefore, neither of the molecules will be soluble in a pH 2.0 phosphate buffer solution. For surfactants, the concentration within the formulations is minimal compared to the macro components for dermatological cream samples, not reaching the threshold of 10 times the concentration of H_2Q.

3.7. Repeatability, reproducibility and stability

To ascertain the repeatability of the prepared sensor and demonstrate the lack of fouling of the modified electrode, the response of $PCVio_{tDES2}$/CNT/GCE was evaluated by DPV in 50.0 μmol L^{-1} H_2Q in 10 replicates leading to a relative standard deviation (RSD%) of 1.08 %, demonstrating excellent repeatability. After 10 scans, no reduction in current peak intensity was observed which evidences the capacity of the PCVio film to avoid electrode fouling by H_2Q. Three $PCVio_{tDES2}$/CNT/GCE were independently prepared in the same conditions for reproducibility evaluation. The RSD% observed for measuring 50.0 μmol L^{-1}

Table 3
Results obtained for recovery tests in dermatological cream samples ($n = 3$).

Pharmaceutical	Found (μmol L^{-1})	Labelled (μmol L^{-1})	Recovery (%)	H_2Q content (mg/g)	
				Electrochemical	Spectrophotometric
Germed	15.2 (±0.2)	15.0	101.3 %	4.1 ± 0.2	4.1 (±0.2)
Hidrospot	15.6 (±0.3)	15.3	101.9 %	4.1 ± 0.2	4.1 (±0.2)

H_2Q in 0.1 mol L^{-1} pH 2.0 phosphate buffer solution was 3.8 % ($n = 3$). Additionally, the response to 50.0 μmol L^{-1} H_2Q was evaluated at a $PCVio_{tDES2}$/CNT/GCE sensor over a 15-day period. The sensor was stored in phosphate buffer 0.1 mol L^{-1} pH 2.0 at 4 °C and kept 88.3 % of its initial electrochemical response after 15 days.

3.8. Pharmaceutical sample analysis

To illustrate practical application, the $PCVio_{tDES2}$/CNT/GCE sensor was employed to analyse the contents of H_2Q in 2 different dermatological creams used for the treatment of melasma, one acquired in a local pharmacy in São Carlos, Brazil (Germed - sample 1) and another acquired in Coimbra, Portugal (Hidrospot - sample 2), by the standard addition method to minimise the influence of the sample matrix. The corresponding plots for analysis of H_2Q in the dermatological creams are shown in Fig. S5. As shown in Table 3, the proposed method presented satisfactory correlation coefficients for both samples, with good recoveries of the H_2Q. The values found (40.6 mg/g – Sample 1 and 40.8 mg/g - Sample 2) were in agreement with the labelled values in the two pharmaceutical leaflets (40 mg/g). The results obtained were compared with those from a spectrophotometric method for the analysis of H_2Q content, described in [36]. Briefly, the cream sample was treated as previously described in Section 2.5 and diluted with appropriate volume of a 0.2 mol L^{-1} H_2SO_4 solution. The H_2Q content was determined using the standard addition method at $\lambda = 287$ nm. The same H_2Q contents obtained by both electrochemical and spectrophotometric methods evidence sensor reliability.

4. Conclusions

A novel electrochemical $PCVio_{tDES2}$/CNT/GCE sensing platform has been proposed, the polymer film based on the electropolymerization of cresyl violet in 1ChCl:1EG:1AcA:1H_2O ternary DES and applied to the detection of H_2Q in dermatological cream samples.

The electropolymerization of CVio sheds new light on the polymerization mechanism of phenazine dyes at CNT in DES. The presence of small amounts of water in the ternary DES promoted the formation of anthraquinone redox couples enhancing the polymer film activity. These conclusions were supported by the CV and EIS data.

The electrochemical properties of PCVio modified electrodes prepared in different binary and ternary DES were investigated by electrochemical techniques and SEM. The best architecture for the detection of H_2Q was the combination of CNT with PCVio film prepared in a H_2SO_4 neutralized ternary DES.

The analytical performance of $PCVio_{tDES2}$/CNT/GCE was evaluated for the determination of H_2Q, showing lower LOD, 0.25 μmol L^{-1}, with a sensitivity of 9.90 μA (μmol L^{-1})$^{-1}$ cm^{-2}. The proposed sensor also showed excellent repeatability, reproducibility and stability, being successfully applied to the detection of H_2Q in dermatological cream samples with very good recoveries.

The new sensor presents a simple architecture, few preparation steps and low cost, evincing the potential use of PCVio-CNT coated electrodes for future application.

CRediT authorship contribution statement

Rafael M. Buoro: Writing – original draft, Investigation, Conceptualization. **Joseany M.S. Almeida:** Writing – review & editing. **Christopher M.A. Brett:** Writing – review & editing, Supervision, Conceptualization.

Declaration of competing interest

The authors declare that they have no known competing financial interests or personal relationships that could have appeared to influence the work reported in this paper.

Data availability

Data will be made available on request.

Acknowledgments

The authors thank Fundação para a Ciência e a Tecnologia (FCT), Portugal, project 2022.06451.PTDC, CEMMPRE, project UIDB/00285/2020 and ARISE, project LA/P/0112/2020 by FEDER funds through the program COMPETE – Programa Operacional Factores de Competitividade, and by national funds through FCT. This study was financed in part by Coordenação de Aperfeiçoamento de Pessoal de Nível Superior – Brasil (CAPES) – Finance Code 001 and by São Paulo Research Foundation (2023/09747–3).

Supplementary materials

Supplementary material associated with this article can be found, in the online version, at doi:10.1016/j.electacta.2024.144305.

References

[1] M.H. Naveen, N.G. Gurudatt, Y.B. Shim, Applications of conducting polymer composites to electrochemical sensors: a review, Appl. Mater. Today 9 (2017) 419–433, https://doi.org/10.1016/j.apmt.2017.09.001.
[2] D. Runsewe, T. Betancourt, J.A. Irvin, Biomedical application of electroactive polymers in electrochemical sensors: a review, Materials 12 (2019) 2629, https://doi.org/10.3390/ma12162629 (Basel).
[3] S. Tajik, H. Beitollahi, F.G. Nejad, I.S. Shoaie, M.A. Khalilzadeh, M.S. Asl, Q. Van Le, K. Zhang, H.W. Jang, M. Shokouhimehr, Recent developments in conducting polymers: applications for electrochemistry, RSC Adv. 10 (2020) 37834–37856, https://doi.org/10.1039/d0ra06160c.
[4] O. Hosu, M.M. Bârsan, C. Cristea, R. Săndulescu, C.M.A. Brett, Nanostructured electropolymerized poly(methylene blue) films from deep eutectic solvents. Optimization and characterization, Electrochim. Acta 232 (2017) 285–295, https://doi.org/10.1016/J.ELECTACTA.2017.02.142.
[5] W. da Silva, A.C. Queiroz, C.M.A. Brett, Nanostructured poly(phenazine)/Fe_2O_3 nanoparticle film modified electrodes formed by electropolymerization in ethaline - deep eutectic solvent. Microscopic and electrochemical characterization, Electrochim. Acta 347 (2020) 136284, https://doi.org/10.1016/J.ELECTACTA.2020.136284.
[6] L. Abad-Gil, C.M.A. Brett, Poly(methylene blue)-ternary deep eutectic solvent/Au nanoparticle modified electrodes as novel electrochemical sensors: optimization, characterization and application, Electrochim. Acta 434 (2022) 285–295, https://doi.org/10.1016/j.electacta.2022.141295.
[7] W. da Silva, C.M.A. Brett, Electrosynthesis and characterisation of novel poly(Nile blue)-deep eutectic solvent/Prussian blue nanoparticle modified electrodes and

their biosensing application, J. Electroanal. Chem. 896 (2021) 115188, https://doi.org/10.1016/j.jelechem.2021.115188.
[8] B. Dalkiran, C.M.A. Brett, Poly(safranine T)-deep eutectic solvent/copper oxide nanoparticle-carbon nanotube nanocomposite modified electrode and its application to the simultaneous determination of hydroquinone and catechol, Microchem. J. 179 (2022) 107531, https://doi.org/10.1016/j.microc.2022.107531.
[9] E.L. Smith, A.P. Abbott, K.S. Ryder, Deep eutectic solvents (DESs) and their applications, Chem. Rev. 114 (2014) 11060–11082, https://doi.org/10.1021/cr300162p.
[10] L.I.N. Tomé, V. Baião, W. da Silva, C.M.A. Brett, Deep eutectic solvents for the production and application of new materials, Appl. Mater. Today 10 (2018) 30–50, https://doi.org/10.1016/J.APMT.2017.11.005.
[11] Q. Zhang, K. De Oliveira Vigier, S. Royer, F. Jérôme, Deep eutectic solvents: syntheses, properties and applications, Chem. Soc. Rev. 41 (2012) 7108–7146, https://doi.org/10.1039/C2CS35178A.
[12] L. Gontrani, N.V. Plechkova, M. Bonomo, In-depth physico-chemical and structural investigation of a dicarboxylic acid/choline chloride natural deep eutectic solvent (NADES): a spotlight on the importance of a rigorous preparation procedure, ACS Sustain. Chem. Eng. 7 (2019) 12536–12543, https://doi.org/10.1021/acssuschemeng.9b02402.
[13] R. Alcalde, A. Gutiérrez, M. Atilhan, S. Aparicio, An experimental and theoretical investigation of the physicochemical properties on choline chloride – lactic acid based natural deep eutectic solvent (NADES), J. Mol. Liq. 290 (2019) 110916, https://doi.org/10.1016/j.molliq.2019.110916.
[14] A.P. Abbott, D. Boothby, G. Capper, D.L. Davies, R.K. Rasheed, Deep eutectic solvents formed between choline chloride and carboxylic acids: versatile alternatives to ionic liquids, J. Am. Chem. Soc. 126 (2004) 9142–9147, https://doi.org/10.1021/JA048266J/SUPPL_FILE/JA048266JSI20040521_085323.PDF.
[15] P.M.V. Fernandes, J.M. Campiña, C.M. Pereira, F. Silva, Electrosynthesis of polyaniline from choline-based deep eutectic solvents: morphology, stability and electrochromism, J. Electrochem. Soc. 159 (2012) G97–G105, https://doi.org/10.1149/2.059209jes.
[16] A.L. Sazali, N. AlMasoud, S.K. Amran, T.S. Alomar, K.F. Pa'ee, Z.M. El-Bahy, T.L. K. Yong, D.J. Dailin, L.F. Chuah, Physicochemical and thermal characteristics of choline chloride-based deep eutectic solvents, Chemosphere 338 (2023) 139485, https://doi.org/10.1016/j.chemosphere.2023.139485.
[17] Y. Dai, J. van Spronsen, G.J. Witkamp, R. Verpoorte, Y.H. Choi, Natural deep eutectic solvents as new potential media for green technology, Anal. Chim. Acta 766 (2013) 61–68, https://doi.org/10.1016/j.aca.2012.12.019.
[18] D.A. Alonso, A. Baeza, R. Chinchilla, G. Guillena, I.M. Pastor, D.J. Ramón, Deep eutectic solvents: the organic reaction medium of the century, European J. Org. Chem. (2016) 612–632, https://doi.org/10.1002/EJOC.201501197, 2016.
[19] D.V. Wagle, H. Zhao, G.A. Baker, Deep eutectic solvents: sustainable media for nanoscale and functional materials, Acc. Chem. Res. 47 (2014) 2299–2308, https://doi.org/10.1021/AR5000488.
[20] L.S.S. Cariati, R.M. Buoro, Evaluation of ionic natural deep eutectic solvents (NADES) modified binders towards the chemical properties of carbon paste electrodes, Electrochem. Commun. 109 (2019) 106605, https://doi.org/10.1016/j.elecom.2019.106605.
[21] A.V. Gómez, A. Biswas, C.C. Tadini, R.F. Furtado, C.R. Alves, H.N. Cheng, Use of natural deep eutectic solvents for polymerization and polymer reactions, J. Braz. Chem. Soc. 30 (2019) 717–726, https://doi.org/10.21577/0103-5053.20190001.
[22] X. Liang, Y. Zhou, J.M.S. Almeida, C.M.A. Brett, A novel electrochemical acetaminophen sensor based on multiwalled carbon nanotube and poly(neutral red) modified electrodes with electropolymerization in ternary deep eutectic solvents, J. Electroanal. Chem. 936 (2023) 117366, https://doi.org/10.1016/j.jelechem.2023.117366.
[23] C.M.A. Brett, Perspectives for the use of deep eutectic solvents in the preparation of electrochemical sensors and biosensors, Curr. Opin. Electrochem. 45 (2024) 101465, https://doi.org/10.1016/j.coelec.2024.101465.
[24] A.S.B. de Sousa, R.P. Lima, M.C.A. da Silva, D. das N. Moreira, M.M.E. Pintado, S. de M. Silva, Natural deep eutectic solvent of choline chloride with oxalic or ascorbic acids as efficient starch-based film plasticizers, Polymer 259 (2022) 125314, https://doi.org/10.1016/j.polymer.2022.125314 (Guildf).
[25] V.I.B. Castro, F. Mano, R.L. Reis, A. Paiva, A.R.C. Duarte, Synthesis and physical and thermodynamic properties of lactic acid and malic acid-based natural deep eutectic solvents, J. Chem. Eng. Data 63 (2018) 2548–2556, https://doi.org/10.1021/acs.jced.7b01037.
[26] O. Zannou, H. Pashazadeh, M. Ghellam, A.Ali Redha, I. Koca, Enhanced ultrasonically assisted extraction of bitter melon (*Momordica charantia*) leaf phenolic compounds using choline chloride-acetic acid–based natural deep eutectic solvent: an optimization approach and *in vitro* digestion, Biomass Convers. Biorefin. (2022), https://doi.org/10.1007/s13399-022-03146-0 online.
[27] P.S. Suresh, P.P. Singh, S.Kapoor Anmol, Y.S. Padwad, U. Sharma, Lactic acid-based deep eutectic solvent: an efficient green media for the selective extraction of steroidal saponins from *Trillium govanianum*, Sep. Purif. Technol. 294 (2022) 121105, https://doi.org/10.1016/j.seppur.2022.121105.
[28] A. Mišan, J. Nađpal, A. Stupar, M. Pojić, A. Mandić, R. Verpoorte, Y.H. Choi, The perspectives of natural deep eutectic solvents in agri-food sector, Crit. Rev. Food Sci. Nutr. 60 (2020) 2564–2592, https://doi.org/10.1080/10408398.2019.1650717.
[29] F.S. Bragagnolo, B. Socas-Rodríguez, J.A. Mendiola, A. Cifuentes, C.S. Funari, E. Ibáñez, Pressurized natural deep eutectic solvents: an alternative approach to agro-soy by-products, Front. Nutr. 9 (2022), https://doi.org/10.3389/fnut.2022.953169.
[30] W. Liu, K. Zhang, J. Chen, J. Yu, Ascorbic acid and choline chloride: a new natural deep eutectic solvent for extracting tert-butylhydroquinone antioxidant, J. Mol. Liq. 260 (2018) 173–179, https://doi.org/10.1016/j.molliq.2018.03.092.
[31] S. Handy, K. Lavender, Organic synthesis in deep eutectic solvents: paal-Knorr reactions, Tetrahedron Lett. 54 (2013) 4377–4379, https://doi.org/10.1016/j.tetlet.2013.05.122.
[32] Y. Zheng, C. Yang, W. Pu, J. Zhang, Determination of oxalic acid in spinach with carbon nanotubes-modified electrode, Food Chem. 114 (2009) 1523–1528, https://doi.org/10.1016/j.foodchem.2008.11.021.
[33] J. Ren, T.F. Kang, R. Xue, C.N. Ge, S.Y. Cheng, Biosensor based on a glassy carbon electrode modified with tyrosinase immmobilized on multiwalled carbon nanotubes, Microchim. Acta 174 (2011) 303–309, https://doi.org/10.1007/S00604-011-0616-1.
[34] M.E. Ghica, R. Pauliukaite, O. Fatibello-Filho, C.M.A. Brett, Application of functionalised carbon nanotubes immobilised into chitosan films in amperometric enzyme biosensors, Sens. Actuators B Chem. 142 (2009) 308–315, https://doi.org/10.1016/j.snb.2009.08.012.
[35] T.A. Silva, H.C.M. Quintão, H. Zanin, E.J. Corat, O. Fatibello-Filho, Amperometric flow injection analysis of hydroquinone in dermatological creams using a porous diamond-like carbon electrode, Diam. Relat. Mater. 139 (2023) 110367, https://doi.org/10.1016/j.diamond.2023.110367.
[36] K.K. de L. Augusto, G.R. Piton, P.C. Gomes-Júnior, G.P. Longatto, F.C. de Moraes, O. Fatibello-Filho, Enhancing the electrochemical sensitivity of hydroquinone using a hydrophobic deep eutectic solvent-based carbon paste electrode, Anal. Methods UK 14 (2022) 2003–2013, https://doi.org/10.1039/D2AY00473A.
[37] J.R. Brusas, E.M.B. Dela Pena, Hygroscopicity of 1:2 choline chloride:ethylene glycol deep eutectic solvent: a hindrance to its electroplating industry adoption, J. Electrochem. Sci. Technol. 12 (2021) 387–397, https://doi.org/10.33961/JECST.2020.01522.
[38] H. Itoi, K. Takagi, T. Usami, Y. Nagai, H. Suzuki, C. Matsuoka, H. Iwata, Y. Ohzawa, Electrochemical oxidation of anthracene to anthraquinone inside the nanopores of activated carbon: implications for electrochemical capacitors, ACS Appl. Nano Mater. 6 (2023) 11541–11552, https://doi.org/10.1021/acsanm.3c01565.
[39] P. Barathi, A.S. Kumar, Electrochemical oxidation of hazardous tetracene to highly redox active anthraquinone and hydroquinone derivatives on a carbon nanotube-modified electrode and its selective hydrogen peroxide sensing, Electroanalysis 26 (2014) 2342–2349, https://doi.org/10.1002/elan.201400250.
[40] D. Połomski, M. Chotkowski, Choline chloride-acetic acid mixture as a medium for the investigation of the electrochemical processes, J. Solid State Electrochem. 28 (2023) 1463–1474, https://doi.org/10.1007/s10008-023-05590-y.
[41] S. Arora, N. Gupta, V. Singh, pH-controlled efficient conversion of hemicellulose to furfural using choline-based deep eutectic solvents as catalysts, ChemSusChem. 14 (2021) 3953–3958, https://doi.org/10.1002/cssc.202101130.
[42] C.M.A. Brett, Electrochemical impedance spectroscopy in the characterisation and application of modified electrodes for electrochemical sensors and biosensors, Molecules 27 (2022) 1497, https://doi.org/10.3390/molecules27051497.
[43] B. Dalkıran, I.P.G. Fernandes, M. David, C.M.A. Brett, Electrochemical synthesis and characterization of poly(thionine)-deep eutectic solvent/carbon nanotube–modified electrodes and application to electrochemical sensing, Microchim. Acta 187 (2020) 609, https://doi.org/10.1007/s00604-020-04588-x.
[44] S. Cotchim, K. Promsuwan, M. Dueramae, S. Duerama, A. Dueraning, P. Thavarungkul, P. Kanatharana, W. Limbut, Development and application of an electrochemical sensor for hydroquinone in pharmaceutical products, J. Electrochem. Soc. 167 (2020) 155528, https://doi.org/10.1149/1945-7111/abd0cd.
[45] T. Chen, J. Xu, M. Arsalan, Q. Sheng, J. Zheng, W. Cao, T. Yue, Controlled synthesis of Au@Pd core-shell nanocomposites and their application for electrochemical sensing of hydroquinone, Talanta 198 (2019) 78–85, https://doi.org/10.1016/j.talanta.2019.01.094.
[46] S. Chuenjitt, A. Kongsuwan, C.H. Phua, J. Saichanapan, A. Soleh, K. Saisahas, K. Samoson, S. Wangchuk, K. Promsuwan, W. Limbut, A poly(neutral red)/porous graphene modified electrode for a voltammetric hydroquinone sensor, Electrochim. Acta 434 (2022) 141272, https://doi.org/10.1016/j.electacta.2022.141272.
[47] H. Huang, Y. Chen, Z. Chen, J. Chen, Y. Hu, J.J. Zhu, Electrochemical sensor based on Ce-MOF/carbon nanotube composite for the simultaneous discrimination of hydroquinone and catechol, J. Hazard. Mater. 416 (2021) 125895, https://doi.org/10.1016/j.jhazmat.2021.125895.
[48] Y. Zhu, S. Huai, J. Jiao, Q. Xu, H. Wu, H. Zhang, Fullerene and platinum composite-based electrochemical sensor for the selective determination of catechol and hydroquinone, J. Electroanal. Chem. 878 (2020) 114726, https://doi.org/10.1016/j.jelechem.2020.114726.
[49] C.C. Maciel, L.F. de Lima, A.L. Ferreira, W.R. de Araujo, M. Ferreira, Development of a flexible and disposable electrochemical sensor based on poly (butylene adipate-co-terephthalate) and graphite for hydroquinone sensing, Sens. Actuators. Rep. 4 (2022) 100091, https://doi.org/10.1016/j.snr.2022.100091.